Modelling of a selforganization process leading to periodic arrays of nanometric amorphous precipitates by ion irradiation

F. Zirkelbach, M. Häberlen, J. K. N. Lindner, and B. Stritzker

Institute of Physics, University of Augsburg, Universitätsstrasse 1, D-86135 Augsburg, Germany

Abstract

Ion irradiation of materials which undergo a drastic density change upon amorphization have been shown to exhibit selforganized, nanometric structures of the amorphous phase in the crystalline host lattice. In order to better understand the process a Monte-Carlo-Simulation code based on a simple model is developed. In the present work we focus on high-dose carbon implantations into silicon. The simulation is able to reproduce results gained by cross-sectional TEM measurements of high-dose carbon implanted silicon. Necessary conditions can be specified for the selforganization process and information is gained about the compositional and structural state during the ordering process which is difficult to be obtained by experiment.

1 Introduction

The formation of nanometric, selforganized, amorphous, lamellar precipitates as a result of high-dose implantation of impurity ions is observed at certain implantation conditions for various ion/target combinations [1-3]. This is surprising since high-dose impurity implantations usually result in the formation of unordered ensembles of precipitates with a broad size distribution [4]. The present work focuses on high-dose carbon implantations into silicon, with doses of $1 - 10 \times 10^{17} cm^{-2}$, an ion energy of $180\,keV$ and substrate temperatures below $400\,^{\circ}\mathrm{C}$ [4,5]. An example of such a lamellar structure is given in the cross-sectional transmission electron microscopy (XTEM) image in Figure 5. A model describing the selforganization process is introduced in this article. This model is used to implement a Monte-Carlo simulation code which reproduces the amorphization and precipitation process. Simulation results will be compared with XTEM measurements. Necessary conditions for creating lamellar precipitates are identified and some additional, difficult-to-gain measure information like the carbon distribution and the influence of stress on the amorphous/crystalline structure in the layers is obtained.

2 Model

A model describing the formation of nanometric, selforganized, regularly arranged, amorphous SiC_x inclusions was introduced in [5]. The basic idea is schematically displayed in Figure 5, giving the evolution into ordered lamellae with increasing dose.

As a result of supersaturation of carbon atoms in silicon at high concentrations there is a nucleation of spherical SiC_x precipitates. Carbon implantations at much higher implantation temperatures usually lead to the precipitation of cubic SiC (3C-SiC, $a = 0.436\,nm$) [4]. The lattice misfit of almost 20% of 3C-SiC would cause a large interfacial energy with the crystalline Si matrix [6]. This energy could be reduced if one of the phases exists in the amorphous state. Energy filtered XTEM studies in [7] have revealed that the amorphous phase is more carbon-rich than the crystalline surrounding. In addition, annealing experiments have shown that the amorphous phase is stable against crystallization at temperatures far above the recrystallization temperature of amorphous Si. Prolonged annealing at 900 °C turns the lamellae into ordered chains of amrphous and crystalline 3C-SiC nanoprecipitates [8] demonstrating again the carbon-rich nature of amorphous inclusions. Since at the implantation conditions chosen pure $a-Si$ would recrystallize by ion beam induced crystallization [9], it is understandable that it is the carbon-rich side of the two phases which occurs in the amorphous state in the present phase separation process.

Stoichiometric SiC has a smaller Si atomic density than $c-Si$ [10,11]. A reduced density is also assumed for substoichiometric $a-SiC_x$. Hence the amorphous SiC_x tends to expand and as a result compressive stress is applied on the Si host lattice represented by arrows in Figure 5. As the process occurs near the target surface, stress is relaxing in the vertical direction and there is mainly lateral stress remaining ("R" in Figure 5). Thus volumes between amorphous inclusions will more likely turn into an amorphous phase as the stress hampers the rearrangement of atoms on regular lattice sites. In contrast, $a-Si$ volumes located in a crystalline neighbourhood will recrystallize in all probability at the present implantation conditions.

Carbon is assumed to diffuse from the crystalline to the amorphous volumes in order to reduce the supersaturation of carbon in the crystalline interstices. As a consequence the amorphous volumes accumulate carbon.

3 Simulation

Before discussing the simulation algorithm some assumptions and approximations have to be made. Figure 5 shows the stopping powers and carbon concentration profiles calculated by TRIM [12]. The depth region we are interested in is between $0 - 300\,nm$ (furtheron called simulation window), the region between the target surface and the beginning of the continuous amorphous SiC_x layer at the implantation conditions of Figure 5. The nuclear stopping power and the implantation profile can be approximated by a linear function of depth within the simulation window.

The target is devided into $64 \times 64 \times 100$ cells with a side length of $3\,nm$. Each of it has a crystalline or amorphous state and keeps the local carbon concentration. The cell is addressed by a position vector $\vec{r} = (k, l, m)$, where k, l, m are integers.

The probability of amorphization is assumed to be proportional to the nuclear stopping power. A local probability of amorphization at any point in the target is composed of three contributions, the ballistic amorphization, a carbon-induced and a stress-induced amorphization. The ballistic amorphization probability p_b is proportional to the nuclear stopping power as mentioned before. The carbon-induced contribution is a linear function of the local carbon concentration. The stress-induced portion is proportional to the compressive stress originating from the amorphous volumes in the vicinity, the stress amplitude decreasing with the square of distance $d = |\vec{r} - \vec{r'}|$. Thus the probability of a crystalline volume getting amorphous can be calculated as

$$p_{c\to a}(\vec{r}) = p_b + p_c\, c_{carbon}(\vec{r}) + \sum_{amorphous\,neighbours} \frac{p_s\, c_{carbon}(\vec{r'})}{d^2} \quad , \tag{1}$$

with p_b, p_c and p_s being simulation parameters to weight the three different mechanisms of amorphization. The probability $p_{a\to c}$ of an amorphous volume to turn crystalline should behave contrary to $p_{c\to a}$ and is thus assumed as:

$$p_{a\to c} = 1 - p_{c\to a} \quad . \tag{2}$$

The simulation algorithm consists of three parts, the amorphization/recrystallization process, the carbon incorporation and finally the carbon diffusion.

For the amorphization/recrystallization process random values are computed to specify the volume which is hit by an impinging carbon ion. Two random numbers $x, y \in [0, 1]$ are generated and mapped to the coordinates k, l using a uniform probability distribution, $p(x)dx = dx$, $p(y)dy = dy$. A random number z corresponding to the m coordinate is distributed according to the linear approximated nuclear stopping power, $p(z)dz = (sz + s_0)dz$, where s and s_0 are simulation parameters describing the nuclear energy

loss. After calculating the local probability of amorphization $p_{c\to a}(k,l,m)$ of the selected volume another random number determines - depending on the current status - whether the volume turns amorphous, recrystallizes or remains unchanged. This step is looped for the average hits per ion in the simulation window as extracted from TRIM [12] collision data.

In the same manner random coordinates are determined to select the cell where the carbon ion gets incorporated. In this step the probability distribution describing the stopping power profile is replaced by a distribution for the linearly approximated concentration profile. The local carbon concentration in the selected cell is increased.

Following carbon incorporation carbon diffusion is considered in order to allow a reduction of the supersaturation of carbon in the crystalline volumes. This is done by a simple diffusion algorithm in which the concentration difference for each two neighbouring cells is considered and partially balanced according to a given diffusion rate d_r (simulation parameter). This time consuming diffusion process is repeated after each d_v (simulation parameter) impinging ions. A switch is implemented to exclude diffusion in z-direction. As in experimental studies diffusional broadening of carbon concentration profiles has not been observed even at significantly higher implantation temperatures where no amorphous phase is formed [13], diffusion among crystalline volumes is assumed to be zero in the following simulations.

4 Results

Figure 5 shows a comparison of a simulation result and a XTEM bright-field image of silicon implanted at 150 °C with 180 keV C^+ ions at a dose of $4.3 \times 10^{17}\, cm^{-2}$. Significant lamellar structure formation is observed in the depth interval between 200 and 300 nm (Figure 4(b)). This is nicely reproduced by the simulation result shown in Figure 4(a). Even the average length of the precipitates complies to the experimental data. The lamellae are arranged in uniform intervals. Obviously the simulation is able to reproduce lamellar, selforganized structures.

Simulations with different model parameters allow to specify conditions for observing lamellar structures. First runs with a simplified version of the program have shown that it is essential to assume low amorphization probabilities to avoid early complete amorphization of the whole cell ensemble. Instead small amorphization parameters p_b, p_c, p_s and a large number of simulation steps are required to observe lamellar structures. This finding is in agreement to the fact that due to the low nuclear energy deposition of the light carbon ions in silicon, amorphization would not be expected at all at these elevated target temperatures [4] and thus carbon mediated amorphization has to be taken into account to explain the amorphization process.

Figure 5 shows the results of two identical simulation runs with diffusion in z-direction switched off and on. The lamellar structures only appear if diffusion in z-direction is enabled. Amorphous volumes denude the neighbouring crystalline layers of carbon. In consequence the stability of such cells against recrystallization is enhanced, the probability to amorphize crystalline cells in the same depth is increased due to the stress term and the amorphization in the carbon denuded cells and their lateral vicinity is decreased. This fortifies the formation of lamellar precipitates. The result highlights the importance of the diffusion in z-direction for the selforganization process.

In Figure 5 two simulation results with different diffusion rates are compared. Higher diffusion rates cause a larger depth domain of lamellar structure. This can be understood since higher diffusion rates result in amorphous volumes holding more carbon which consequently stabilizes the amorphous state. In case of slower diffusion rates (Figure 6(b)) the redistribution of carbon is too slow to allow for an effective agglomeration of carbon atoms in amorphous cells to stabilize the amorphous state against recrystallization. This results in a smaller total amount of amorphous material in Figure 6(a) compared to Figure 6(b). The stabilization occurs only at a depth larger than approximately 240 nm where the total concentration of carbon is high enough. The sufficient stabilization of amorphous volumes in this deeper depth zone enables also the more effective contribution

of the stress mediated amorphization.

The influence of the stress term p_s is considered in Figure 5. For otherwise the same conditions as in Figure 6(b) calculations with decreased p_s in Figure 7(c),(b),(a) show a systematically reduced extension of the lamellae zone. The mean diameter of amorphous lamellae decreases with decreasing p_s. Both observations support the assumption of stress mediated amorphization as a mechanism contributing to lamella formation.

Figure 5 shows the extension of amorphous lamellae in plane view for two consecutive slices m and $m+1$ of the ensemble. It is obvious that amorphous and crystalline lamellae have a complementary arrangement in neighbouring slices (Figure 8(a),(b)) which again is a result of the carbon accumulation in the amorphous lamellae. This can be clearly seen by comparison with the corresponding carbon maps in Figure 8(c),(d).

5 Summary and conclusion

A simple model explaining the selforganization process of lamellar, amorphous precipitates during high-dose ion implantation is introduced. The implementation of the model in a simulation code is described. The simulation is able to reproduce the experimentally observed formation of lamellae. The evolution of these lamellar structures gets traceable by the simulation. The weight of different mechanisms which contribute to the selforganization process is explored by variation of simulation parameters. It is found that diffusion in z-direction and stress mediated amorphization are necessary to create ordered arrays of amorphous, lamellar precipitates. Thus by simulation, information is gained about the selforganization process which is not easily accessible by experimental techniques.

References

[1] L.L. Snead, S.J. Zinkle, J.C. Hay, M.C. Osborne, Nucl. Instr. and Meth. B 141 (1998) 123.

[2] A.H. van Ommen, Nucl. Instr. and Meth. B 39 (1989) 194.

[3] M. Ishimaru, R.M. Dickerson, K.E. Sickafus, Nucl. Instr. and Meth. B 166-167 (2000) 390.

[4] J.K.N. Lindner, Appl. Phys. A 77 (2003) 27-38.

[5] J.K.N. Lindner, M. Häberlen, M. Schmidt, W. Attenberger, B. Stritzker, Nucl. Instr. and Meth. B 186 (2000) 206-211.

[6] W.J. Taylor, T.Y. Tan, U.Gösele, Appl. Phys. Lett. 62 (1993) 3336.

[7] M. Häberlen, J.K.N. Lindner, B. Stritzker, to be published.

[8] M. Häberlen, J.K.N. Lindner, B. Stritzker, Nucl. Instr. and Meth. B 206 (2003) 916-921.

[9] J. Linnross, R.G. Elliman, W.L. Brown, J. Mater, Res. 3 (1988) 1208.

[10] L. L. Horton, J. Bentley, L. Romana, A. Perez, C.J. McHargue, J.C. McCallum, Nucl. Intr. and Meth. B 65 (1992) 345.

[11] W. Skorupa, V. Heera, Y. Pacaud, H. Weishart, in: F. Priolo, J.K.N. Lindner, A. Nylandsted Larsen, J.M. Poate (Eds.), New Trends in Ion Beam Processing of Materials, Europ. Mater. Res. Soc. Symp. Proc. 65, Part 1, Elsevier, Amsterdam, 1997, p. 114.

[12] SRIM2000 Version of the TRIM program described by J.F. Ziegler, J.P. Biersack, U. Littmark in: The Stopping and Range of Ions in Matter, vol. 1, Pergamon Press, New York, 1985.

[13] J.K.N. Lindner, W. Reiber, B. Stritzker, Mater. Sci. Forum Vols. 264-268 (1998) 215-218.

Figure Captions

1. XTEM image of a Si sample implanted with $180\,keV\,C^+$ ions at a dose of $4.3 \times 10^{17}\,cm^{-2}$ and a substrate temperature of 150 °C. Lamellar and spherical amorphous inclusions are marked by L and S.

2. Schematic explaining the selforganization of amorphous SiC_x precipitates and the evolution into ordered lamellae with increasing dose (see text).

3. Nuclear and electronic stopping powers and concentration profile of $180\,keV\,C^+$ ions implanted in Si calculated by TRIM.

4. Comparison of a simulation result and a XTEM image ($180\,keV\ C^+$ implantation into silicon at 150 °C and a dose of $4.3 \times 10^{17} cm^{-2}$). Amorphous cells are white.

5. Two identical simulation runs with diffusion switched off (left) and on (right).

6. Two identical simulation runs with different diffusion rates d_r. All other parameters are as in Figure 5(b).

7. Four simulation runs with different simulation parameter p_s. All other parameters are as in Figure 5(b).

8. Plane view display of amorphous (white) and crystalline (black) cells in two consecutive slices m and $m+1$ (a,b) and corresponding carbon map (c,d). Higher carbon concentrations are given by higher brightness in (c,d).

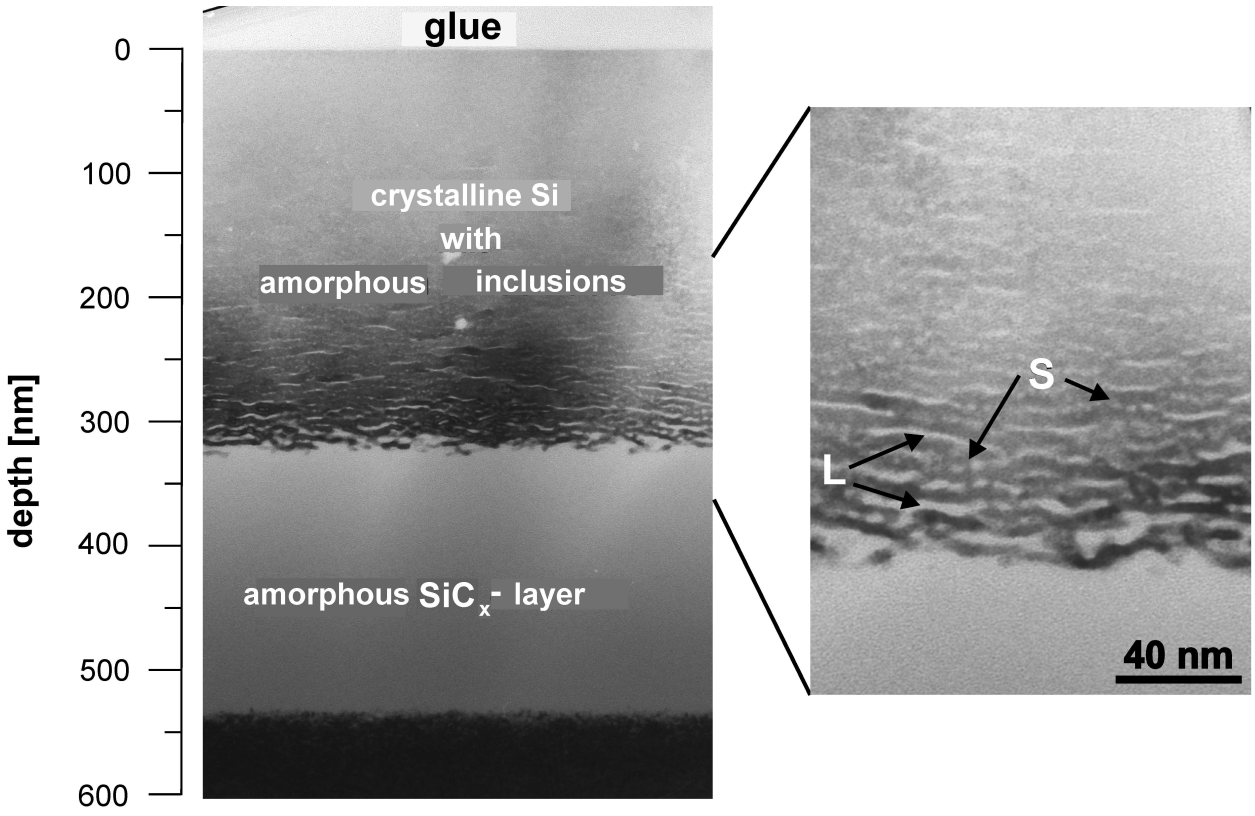
glue
0
100
200
300
400
500
600
depth [nm]
crystalline Si
with
amorphous inclusions
amorphous SiC$_x$- layer
S
L
40 nm

1

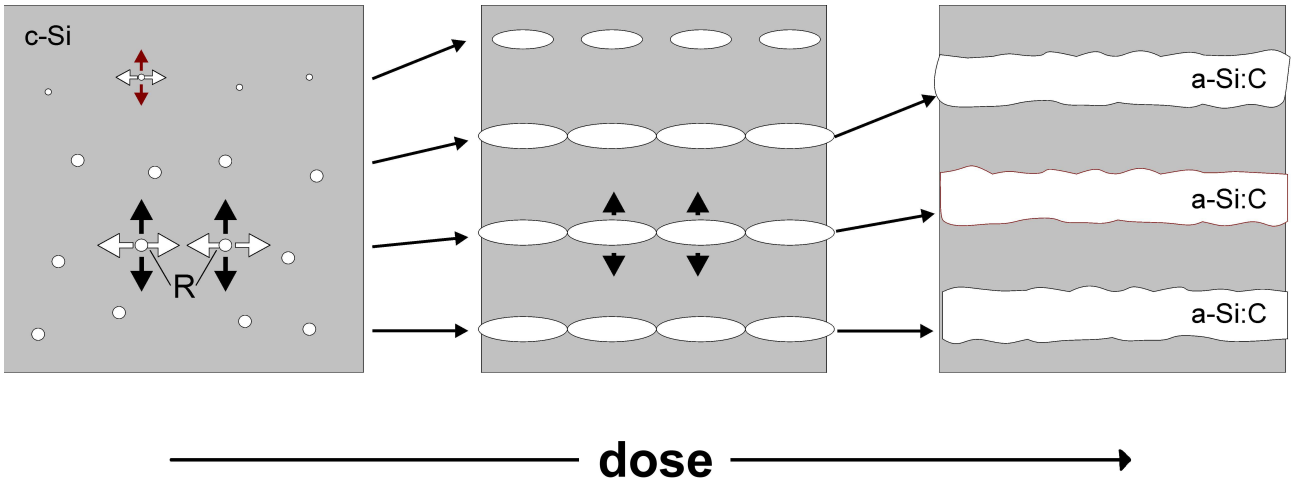
c-Si
R
a-Si:C
a-Si:C
a-Si:C
dose

2

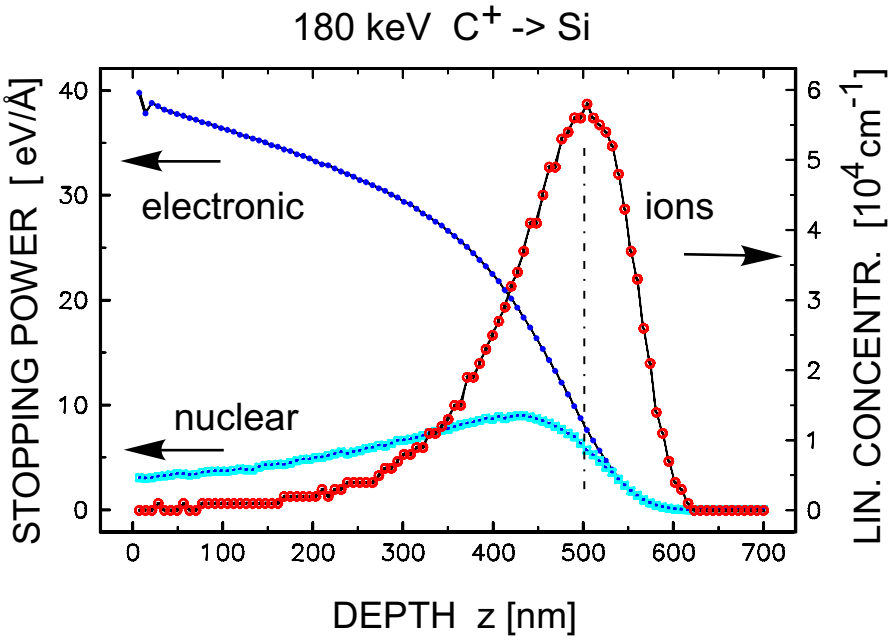
180 keV C+ -> Si
STOPPING POWER [eV/Å]
LIN. CONCENTR. [10^4cm^-1]
electronic
nuclear
ions
DEPTH z [nm]
0
10
20
30
40
0
1
2
3
4
5
6
0
100
200
300
400
500
600
700

.

3

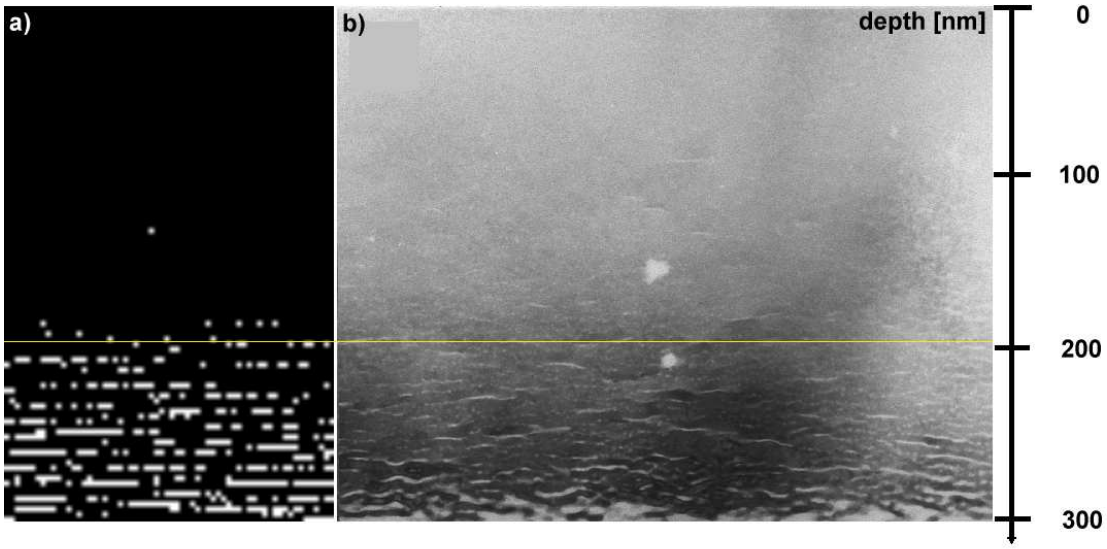
a)
b)
depth [nm]
0
100
200
300

4

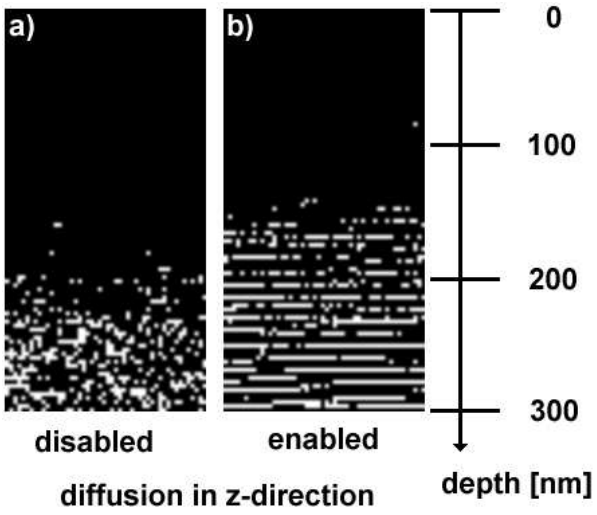
a)
b)
0
100
200
300
disabled
enabled
diffusion in z-direction
depth [nm]

5

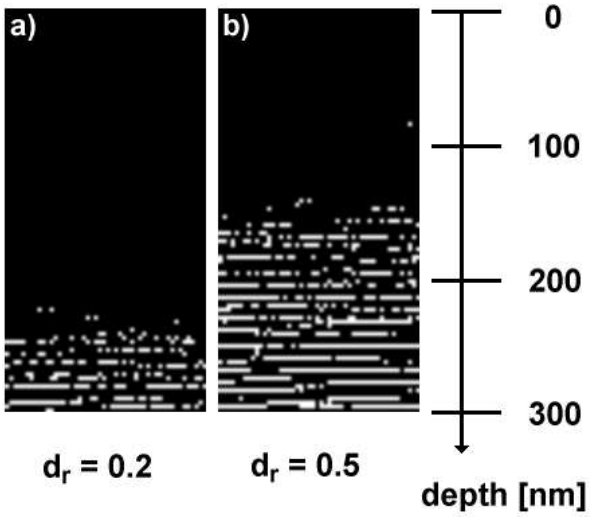
a)
b)
0
100
200
300
d_r = 0.2
d_r = 0.5
depth [nm]

6

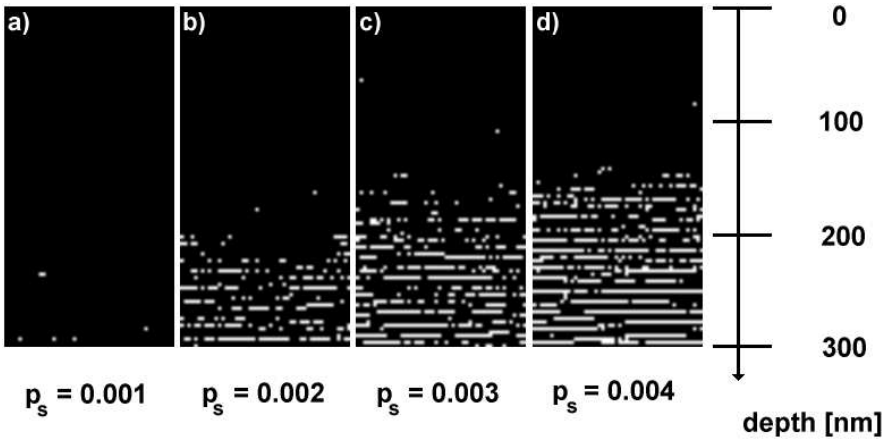
a)
b)
c)
d)
0
100
200
300
p_s = 0.001
p_s = 0.002
p_s = 0.003
p_s = 0.004
depth [nm]

7

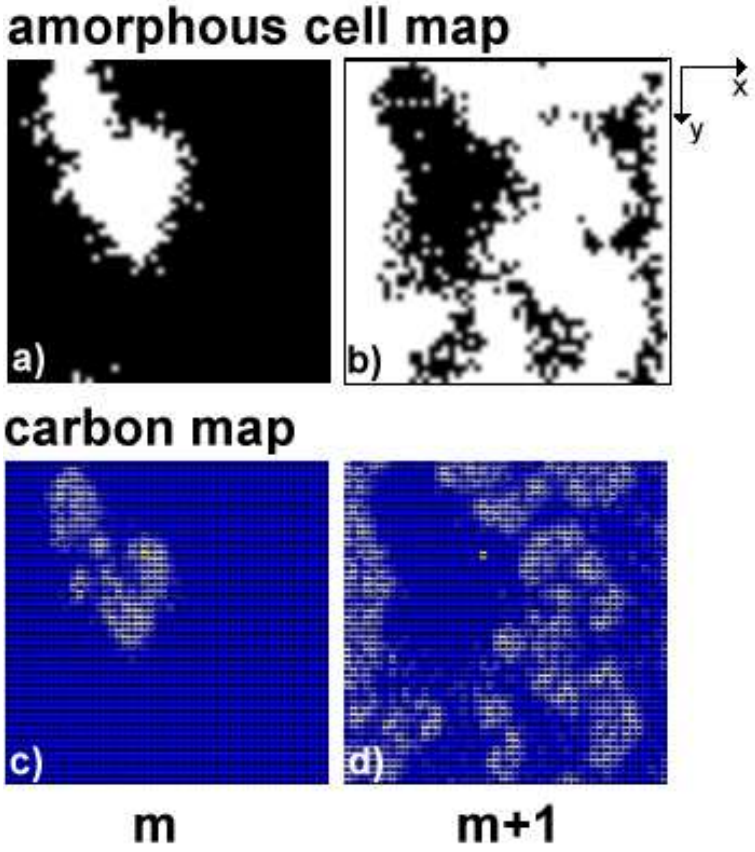

8